APPROXIMATION OF CRYSTALLINE DENDRITE GROWTH IN TWO SPACE DIMENSIONS

A. SCHMIDT

ABSTRACT. The phase transition between solid and liquid in an undercooled liquid leads to dendritic growth of the solid phase. The problem is modelled by the Stefan problem with a modified Gibbs-Thomson law, which includes the anisotropic mean curvature corresponding to a surface energy that depends on the direction of the interface normal. A finite element method for discretization of the Stefan problem is described which is based on a weak formulation of the anisotropic mean curvature flow. Numerical experiments with a nearly crystalline anisotropy are presented.

INTRODUCTION

Phase transition between liquid and solid phase with dendritic growth of the solid phase inside an undercooled liquid can be modeled by the Stefan problem with a modified Gibbs-Thomson law which accounts for anisotropic surface tension and kinetic undercooling [**8**].

We denote by $\theta(x,t)$ the temperature in a domain $\Omega \subset \mathbf{R}^n$ and by $\Gamma(t)$ the moving free boundary with normal velocity V and anisotropic mean curvature C_α. The sign of these two scalar quantities is chosen such that for a growing convex solid, both V and C_α are positive. Let ν denote the outer normal to the solid region. The system of equations consists of the heat equation (1) in both solid and liquid regions, the Stefan condition (2), and the Gibbs-Thomson relation (3). Assuming for simplicity unit thermal conductivities in both phases and unit latent heat, the system reads

$$\theta_t - \Delta\theta = 0 \qquad \text{in } \Omega \setminus \Gamma(t), \tag{1}$$

$$\left[\frac{\partial\theta}{\partial\nu}\right] + V = 0 \qquad \text{on } \Gamma(t), \tag{2}$$

$$\theta + \beta(\nu)V + C_\alpha = 0 \qquad \text{on } \Gamma(t), \tag{3}$$

together with initial conditions for θ and Γ as well as boundary conditions for the temperature. We assume that Γ does not meet the domain's boundary and

will not change its topology but stays equivalent to the initial interface, like a sphere S^{n-1}.

The modified Gibbs-Thomson relation (3) enables the growth of dendritic structures, as it incorporates the influence of an anisotropic mobility and an anisotropic interface energy, which can be motivated by the underlying crystalline structure of the solid. For this reason one assumes that the kinetic coefficient β and the interface energy depend only on the direction of the surface normal ν. This is appropriate for the case of single solid crystals. Besides the normal velocity of the interface, the Gibbs-Thomson relation includes an **anisotropic mean curvature** (or **weighted mean curvature**) C_α, which reduces to the mean curvature of the interface (scaled by some material constant) in the case of constant isotropic interface energy.

Taylor [12] compares several different formulations of (weighted) mean curvature for smooth and crystalline anisotropy, however, a weak formulation which is well suited for manifolds of weak regularity (only Lipschitz or H^1) and a finite element approximation is not directly included. In [13], geometric models for crystal growth based on these curvature formulations are presented. Bellettini and Paolini [3] treat mean curvature flow in the context of Finsler geometries, where not only the interface but also the surrounding space exhibits some anisotropic structure. This leads to somewhat different equations. Rybka considers the Stefan problem with purely crystalline interface motion and studies existence and uniqueness of solutions as well as asymptotic behaviour for vanishing solid phase.

Dziuk [4] uses a weak formulation of the mean curvature for a finite element approximation of motion by mean curvature. Convergence of the semidiscrete method for curves (discretized in space) was shown in [5]. Recently, this convergence result was extended to the case of smooth anisotropies [6].

In [2], [11] we presented a finite element method for the approximation of dendritic growth in two and three space dimensions, where we use a Gibbs-Thomson law of the form

$$\theta + \beta(\nu)V + \alpha(\nu)C_\Gamma = 0 \qquad \text{on } \Gamma(t),$$

where C_Γ is the usual mean curvature. This includes the general case of weighted mean curvature for smooth anisotropies in two dimensions, but not in three dimensions. The method is based on Dziuk's discretization of mean curvature evolution [4]. Recently, Veeser [14] proved convergence and error estimates for the corresponding semidiscretization in space in two dimensions.

Here we consider the twodimensional situation and describe the extension of the above mentioned finite element method to the case of true anisotropic interface energy which enables the finite element approximation of the general weighted mean curvature case also in three dimensions as well as the consideration of non smooth anisotropies. First numerical results for nearly crystalline anisotropy in two space dimensions are presented.

1. Motion by Anisotropic Curvature

In this section we study the first variation of the anisotropic surface energy, which is connected to the motion by anisotropic mean curvature via the corresponding gradient flow.

Let Γ be a smooth closed curve embedded in $\mathbf{R}^2$ and ν the outer unit normal vector field on Γ. The isotropic surface energy E (or measure) of Γ is given by

$$E(\Gamma) := \int_\Gamma 1 \, do.$$

The first variation of E involves the mean curvature C_Γ of Γ, as we will see below, and the mean curvature flow is the gradient flow for E. Motion by anisotropic curvature can be derived in a similar way, as we describe now. Given an anisotropic surface energy weight function $\alpha : S^1 \to \mathbf{R}$, $\alpha > 0$, which depends only on the normal direction, the anisotropic surface energy $E_\alpha(\Gamma)$ is defined as

$$E_\alpha(\Gamma) := \int_\Gamma \alpha(\nu) \, do.$$

Let α be extended 1-homogeneously to the whole $\mathbf{R}^2$ such that $\alpha(\lambda\nu) = \lambda\alpha(\nu)$ for all $\lambda \geq 0$. We want to derive weak formulas of the first variation of E_α and the corresponding gradient flow.

Let Γ be given via a periodic parametrization $x : I \subset \mathbf{R} \to \mathbf{R}^2$ with $do(x_s) = |x_s| > 0$ the surface element at x and $\nu(x_s) = x_s^\perp / |x_s|$ the unit normal to Γ (where $\perp$ denotes rotation by $-\pi/2$). For a periodic perturbation $\varphi : I \to \mathbf{R}^2$ of x, the first variation of $E_\alpha(x) := E_\alpha(\Gamma)$ in direction of φ is

$$
\begin{aligned}
\langle\!\langle E_\alpha'(x), \varphi \rangle\!\rangle &= \left.\frac{d}{d\varepsilon}\right|_{\varepsilon=0} E_\alpha(x + \varepsilon\varphi) \\
&= \left.\frac{d}{d\varepsilon}\right|_{\varepsilon=0} \int_I \alpha(\nu(x_s + \varepsilon\varphi_s)) \, do(x_s + \varepsilon\varphi_s) \\
&= \int_I D\alpha(\nu(x_s)) \cdot D\nu(x_s) \cdot \varphi_s \, do(x_s) + \alpha(\nu(x_s)) \, D(do)(x_s) \cdot \varphi_s \,,
\end{aligned}
$$

where we only used the chain rule. The gradient $D\alpha(\nu)$ is sometimes called "Cahn-Hoffman ξ-vector" in the literature.

Using the explicit formulas for ν and do, the variation can be expressed in the following way (where $\langle \cdot, \cdot \rangle$ denotes the euclidian scalar product of vectors in $\mathbf{R}^2$):

$$
\begin{aligned}
\langle\!\langle E_\alpha'(x), \varphi \rangle\!\rangle &= \int_I \left\langle D\alpha\Big(\frac{x_s^\perp}{|x_s|}\Big), \varphi_s^\perp - \frac{x_s^\perp}{|x_s|^2}\langle\varphi_s, x_s\rangle \right\rangle + \alpha\Big(\frac{x_s^\perp}{|x_s|}\Big)\left\langle \frac{x_s}{|x_s|}, \varphi_s \right\rangle \\
&= \int_I \left(\left\langle D\alpha\Big(\frac{x_s^\perp}{|x_s|}\Big), \frac{x_s}{|x_s|} \right\rangle \left\langle \frac{x_s}{|x_s|}, \frac{\varphi_s^\perp}{|x_s|} \right\rangle + \alpha\Big(\frac{x_s^\perp}{|x_s|}\Big)\left\langle \frac{x_s}{|x_s|}, \frac{\varphi_s}{|x_s|} \right\rangle \right) |x_s| \,,
\end{aligned}
$$

since $\varphi_s^\perp - \frac{x_s^\perp}{|x_s|}\langle\varphi_s, \frac{x_s}{|x_s|}\rangle = \varphi_s^\perp - \frac{x_s^\perp}{|x_s|}\langle\varphi_s^\perp, \frac{x_s^\perp}{|x_s|}\rangle = \frac{x_s}{|x_s|}\langle\varphi_s^\perp, \frac{x_s}{|x_s|}\rangle$. This leads to the following non parametric formulation for a perturbation $\varphi : \Gamma \to \mathbf{R}^2$:

$$(4) \qquad \langle\!\langle E_\alpha'(\Gamma), \varphi \rangle\!\rangle = \int_\Gamma \Big(\langle D\alpha(\nu), \underline\nabla\mathrm{id}\rangle \, \langle\underline\nabla\mathrm{id}, \underline\nabla\varphi^\perp\rangle + \alpha(\nu)\langle\underline\nabla\mathrm{id}, \underline\nabla\varphi\rangle \Big)\, do,$$

where $\underline\nabla$ is the tangential gradient (or covariant derivative) on Γ and $\mathrm{id}\colon \Gamma \to \mathbf{R}^2$ is the identity vector field on $\mathbf{R}^2$ (the embedding of Γ). This formulation is well suited for an isoparametric finite element discretization, see Section 2.

In the isotropic case, $\alpha = \mathrm{const}$, integration by parts gives on closed curves or for perturbations which vanish on $\partial\Gamma$

$$\langle\!\langle E_\alpha'(\Gamma), \varphi \rangle\!\rangle \;=\; -\alpha \int_\Gamma \langle\underline\Delta\mathrm{id}, \varphi\rangle\, do,$$

where $\underline\Delta$ is the Laplace-Beltrami operator on Γ. Now, $\underline\Delta\mathrm{id}$ is just the mean curvature vector $\vec{C}_\Gamma$ of Γ, which gives $E_\alpha'(\Gamma) = -\alpha\vec{C}_\Gamma$. Thus, the gradient flow for E_α is in the isotropic case just mean curvature flow $\vec{V} = \alpha\vec{C}_\Gamma$, where the velocity of a moving manifold is equal to α times mean curvature. With the given sign convention for the scalar quantities V and C_Γ, it holds $\nu V = \vec{V} = \alpha\vec{C}_\Gamma = -\alpha\nu C_\Gamma$.

Similarly, the gradient flow for anisotropic surface energy is the anisotropic curvature flow (or weighted mean curvature flow)

$$\int_\Gamma \langle\vec{V}, \varphi\rangle\, do = \langle\!\langle E_\alpha'(\Gamma), \varphi\rangle\!\rangle$$

for all smooth perturbations φ, and with

$$\vec{C}_\alpha := E_\alpha'(\Gamma),$$

we have the anisotropic curvature flow equation

$$\vec{V} = \vec{C}_\alpha\,.$$

Depending on the smoothness of α and Γ, this equation holds only in a weak sense. For smooth α it is easy to show that this leads (for curves) to $\vec{V} = (\tilde\alpha + \tilde\alpha'')\vec{C}_\Gamma$, if $\alpha(\nu) = \tilde\alpha(\gamma)$, where $\gamma = \angle(\nu, e_1)$ is the angle between the normal and the e_1 coordinate axis.

The connection between anisotropic curvature flow $\vec{V} = \vec{C}_\alpha$ and the Gibbs-Thomson relation $\beta V = -C_\alpha - \theta$ is given after conversion to scalar quantities (by multiplying with $\pm\nu$, such that the scalar mean curvature for a convex solid phase is positive, and the scalar velocity for an expanding solid is positive), and by using the temperature as an additional forcing term.

Using the 1-homogeneity of α, we can derive a simpler expression for the first variation, which is not so well suited for a finite element formulation of anisotropic mean curvature flow like (4), but can be used to evaluate the anisotropic curvature.

$$\langle\!\langle E'_\alpha(x), \varphi \rangle\!\rangle = \frac{d}{d\varepsilon}\Big|_{\varepsilon=0} \int_I \alpha(x_s^\perp + \varepsilon\varphi_s^\perp) = \int_I \langle D\alpha(x_s^\perp), \varphi_s^\perp\rangle$$
$$= \int_I \left\langle D\alpha\left(\frac{x_s^\perp}{|x_s|}\right), \frac{\varphi_s^\perp}{|x_s|}\right\rangle |x_s|,$$

which leads to the intrinsic equation

(5)
$$\langle\!\langle E'_\alpha(\Gamma), \varphi \rangle\!\rangle = \int_\Gamma \langle D\alpha(\nu), \underline{\nabla}\varphi^\perp\rangle \, do\,.$$

Wulff Shapes For a given anisotropy α, the Wulff shape $\mathcal{W}_\alpha$ is defined as

$$\mathcal{W}_\alpha = \big\{x \in \mathbf{R}^n \mid \langle x, \nu\rangle \leq \alpha(\nu) \ \forall\, \nu \in S^{n-1}\big\}.$$

It is known that anisotropic curvature flow of an initially convex curve converges to a self-similarly shrinking Wulff shape [**7**]. If the polar graph of $1/\alpha$ (the Frank diagram) is strictly convex (i.e. $\tilde\alpha + \tilde\alpha'' > 0$), then $\mathcal{W}_\alpha$ is strictly convex, too. For crystalline anisotropies of k-fold symmetry,

(6)
$$\tilde\alpha_k(\gamma) = \varepsilon \, \max\big\{\cos(\gamma - 2\pi j/k);\ j = 0, \ldots, k-1\big\},$$

$\tilde\alpha_k + \tilde\alpha_k''$ is concentrated at discrete angles and vanishes almost everywhere, and the corresponding Wulff shape is a regular k-polygon. For crystalline curvature flow without driving forces, the Wulff shape faces are the only directions which appear in an evolving manifold. We will see in the numerical results that Wulff shape faces are preferred in the free boundary problem, too.

2. A Finite Element Method for Dendrite Growth

Let $V_h \subset H^1(\Omega)$ and $V_{h,0} = V_h \cap H_0^1(\Omega)$ be finite element spaces of continuous piecewise polynomial functions on a regular triangulation of Ω. After time discretization with time step size $\tau_m = t_m - t_{m-1}$, we denote by $\theta_h^m \in V_h$ the discrete temperature and by Γ_h^m a continuous, piecewise polynomial discrete interface at time t_m. Let $W_h^m \subset H^1(\Gamma_h^m)$ be the isoparametric finite element space of piecewise polynomial functions on Γ_h^m. The discretization of the interface is totally independent from the temperature mesh, and coupling between both is only done via integrals over the free boundary.

For discretization of the interface evolution, we proceed according to [**4**] by parametrizing Γ_h^m over Γ_h^{m-1} via $x_h^m \colon \Gamma_h^{m-1} \to \mathbf{R}^2$, $x_h^m \in (W_h^{m-1})^2$. After multiplying the Gibbs-Thomson relation (3) by the normal ν in order to get a vector

valued equation, we use equation (4) for a variational formulation and derivation of a finite element method. This leads to a highly nonlinear equation for x_h^m, as the normal ν^m (which is a parameter to α and $D\alpha$) and the tangential derivative $\underline{\nabla}$ on Γ_h^m all depend on the parametrization. To avoid this nonlinear problem, we use a linearization which uses the normal vector field ν^{m-1} and tangential derivatives $\underline{\nabla}$ corresponding to the old interface Γ_h^{m-1}. This leads to the following semi-implicit, linearized problem for $x_h^m \in (W_h^{m-1})^2$:

$$\int_{\Gamma_h^{m-1}} \beta \frac{x_h^m - \mathrm{id}}{\tau_m}\, \varphi_h + \langle D\alpha(\nu^{m-1}), \underline{\nabla}\mathrm{id}\rangle\langle \underline{\nabla}x_h^m, \underline{\nabla}\varphi_h^\perp\rangle + \alpha(\nu^{m-1})\,\langle \underline{\nabla}x_h^m, \underline{\nabla}\varphi_h\rangle$$

$$= -\int_{\Gamma_h^{m-1}} \theta_h^{m-1}\langle \nu^{m-1}, \varphi_h\rangle, \qquad \forall\varphi_h \in (W_h^{m-1})^2.$$

As we are using isoparametric finite elements, we can define the new discrete interface by

$$\Gamma_h^m := x_h^m(\Gamma_h^{m-1}).$$

After integration by parts in the solid and liquid subdomains with a test function $\psi_h \in V_h$, the heat equation (1) leads to a parabolic problem for $\theta_h^m \in V_h$ with a right hand side given by a line integral:

$$\int_\Omega \frac{\theta_h^m - \theta_h^{m-1}}{\tau_m}\, \psi_h + \langle\nabla\theta_h^m, \nabla\psi_h\rangle = \int_{\Gamma_h^m} V\psi_h, \qquad \forall\psi_h \in V_h.$$

We use the Gibbs-Thomson relation (3) to replace the velocity V and get

$$\int_\Omega \frac{\theta_h^m - \theta_h^{m-1}}{\tau_m}\, \psi_h + \langle\nabla\theta_h^m, \nabla\psi_h\rangle + \int_{\Gamma_h^m} \frac{1}{\beta}\theta_h^m\psi_h = -\int_{\Gamma_h^m} \frac{1}{\beta}C_\alpha\psi_h, \qquad \forall\psi_h \in V_h,$$

which gives a more stable discretization by including the temperature at the interface implicitly. The right hand side is evaluated by calculating $\langle\langle \vec{C}_\alpha, \frac{1}{\beta}\psi_h\nu\rangle\rangle = \langle\langle E_\alpha'(\Gamma_h^m), \frac{1}{\beta}\psi_h\nu\rangle\rangle$. Instead of using here (4), we can take advantage of the simpler expression (5).

The two finite element methods described above are coupled to a method for simulation of the free boundary problem. The simplest coupling is the following: In each time step, the coupled method first computes the new discrete interface Γ_h^m using the old temperature θ_h^{m-1}. The new temperature θ_h^m is then computed by using this new interface. More elaborate couplings are possible, using extrapolation techniques or higher order time discretizations.

Adaptive Methods. Instead of using one single finite element space V_h for all time steps, the triangulation is adapted to the actual solution based on a posteriori

error indicators and local refinement and coarsening of the mesh, see [**11**]. This leads to finite element spaces V_h^m for the discrete temperature θ_h^m. An additional mesh transfer operator I_h^m is needed in order to project the old temperature θ_h^{m-1} from V_h^{m-1} to the new space. For adaptive modifications of the temperature mesh, we use local refinement and coarsening of triangles based on bisection methods [**1**]. This leads to compatible triangulations after mesh changes such that an interpolation error $|\theta_h^{m-1} - I_h^m \theta_h^{m-1}| > 0$ is introduced only during coarsening, not by local refinement operations.

The interface discretization has to be adapted, too. During the evolution, large parts of the interface can grow out of initially small interface regions. For curves, this adaption can be done by bisecting polygon pieces, which grow longer than a specified threshold length. This simple criterion generates usually good numerical results. More elaborate error indicators for local adaption of the polygon can be derived.

3. Numerical Simulations with Nearly Crystalline Anisotropy

Simulations with smooth anisotropy were presented in [**2**], [**11**]. Our aim here is to approximate dendritic growth with the crystalline anisotropy $\alpha_k(\nu)$ given in terms of $\tilde{\alpha}_k(\gamma)$, compare (6).

The equation for anisotropic mean curvature flow (4) makes sense if Γ is Lipschitz, because then the Sobolev space $H^1(\Gamma)$ is well defined [**15**] and $\mathrm{id}|_\Gamma \in H^1(\Gamma)$ holds. The Lipschitz continuity of our discrete interfaces Γ_h^m is guaranteed by the definition via piecewise polynomial continuous parametrizations. For the anisotropy, additional regularity is needed in order to be able to evaluate $\alpha(\nu)$ and $D\alpha(\nu)$. As Γ is only Lipschitz, the normal vector field ν is only L^∞; the discrete normal ν^m is piecewise smooth but jumps at discrete points. For integration of $D\alpha(\nu)$, we now need $\alpha \in C^1$-regularity. This means that the crystalline anisotropy α_k, which is only Lipschitz, can not be used directly.

We use a periodic regularization $\tilde{\alpha}_{k,\delta}(\gamma) \in C^1(\mathbf{R})$ which is defined in the following way. Set

$$\tilde{\alpha}_{k,\delta}(\gamma) = \delta + \begin{cases} \tilde{\alpha}_k(\gamma) & \text{if } \left|\gamma - \dfrac{(2j+1)\pi}{k}\right| > \delta, \ j = 0, \ldots, k-1, \\ p(\gamma) & \text{otherwise,} \end{cases}$$

where $\delta > 0$ is the regularization parameter and $p(\gamma)$ are pieces of quadratic polynomials such that $\tilde{\alpha}_{k,\delta} \in C^1$ holds, see Figure 1. Corresponding Wulff shapes are shown in Figure 2. The simulations presented below were done with $\delta = 0.1$.

Numerical results. We present results from two simulations. Both are done with piecewise quadratic finite element discretizations of the temperature and the
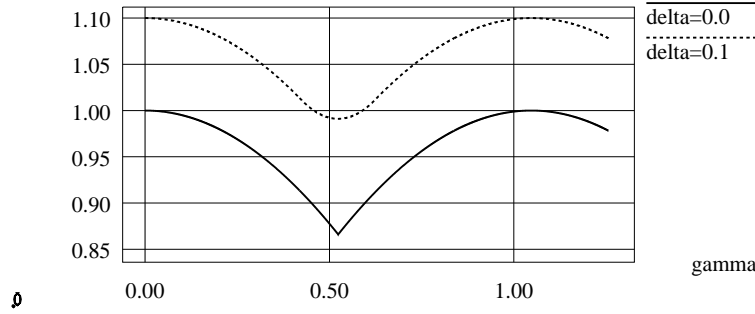
Figure 1. Crystalline anisotropy $\tilde{\alpha}_6$ (solid) and regularization
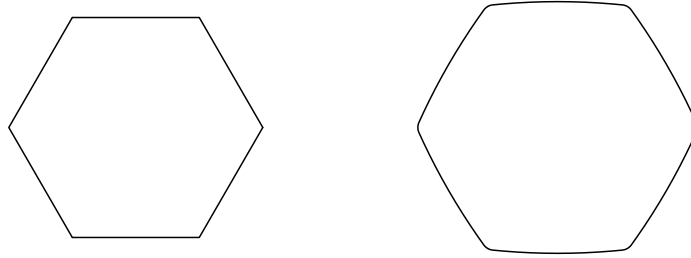$\tilde{\alpha}_{6,\delta}$ (dotted) for $\delta = 0.1$.

Figure 2. Wulff shapes for crystalline anisotropy $\tilde{\alpha}_6$ (left)
and regularization $\tilde{\alpha}_{6,0.1}$ (right).

interface curve. The domain is $\Omega = (-4, +4)^2$, the initial curve is a circle of
radius $R_0 = 0.1$. The anisotropic coefficients in the Gibbs-Thomson relation are
$\alpha = 0.001 \, \alpha_{6,0.1}$ and $\beta(\nu) = 0.01$ (isotropic kinetic coefficient). Boundary value
for the temperature is $\theta = -0.5$ on $\partial\Omega$.

    In the first simulation, the parameter for temperature mesh adaption is $tol =$
0.02. We use a fixed time step size of $\tau = 0.00025$. The simulation runs over a time
interval $[0, 2.25]$ of 9000 time steps. The curve pieces are allowed to have a length of
0.005, with bisection refinement if they grow longer. Figure 3 shows the evolving
interface at time $t = 0.0, 0.25, 0.5, \ldots, 2.25$ (after $0, 1000, \ldots, 9000$ time steps).
The outer square depicts the domain boundary $\partial\Omega$. In Figure 4, a zoom to the
upper right part of the interfaces is shown. It shows clearly that the Wulff shape
faces are preferred directions for the interface, too. But in regions of high velocity,
especially near the dendrite tips, where the temperature is more negative and thus
the forcing term in the mean curvature equation is larger, intermediate directions
appear, too. Zooms of the locally adapted temperature meshes at $t = 0.25, 2.0$ are
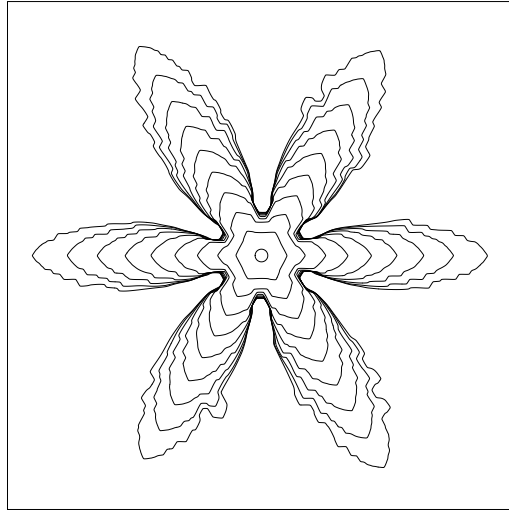shown in Figures 5 and 6.

Figure 3. Example 1 – Interface curves at $t = 0.0, 0.25, 0.5, \ldots, 2.25$.
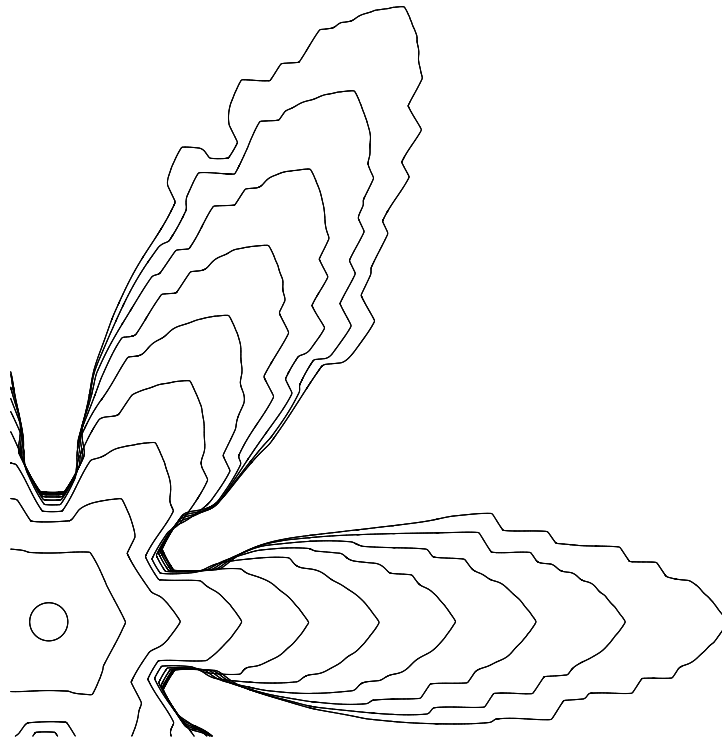

Figure 4. Example 1 – zoom of interface curves at $t = 0.0, 0.25, 0.5, \ldots, 2.25$.
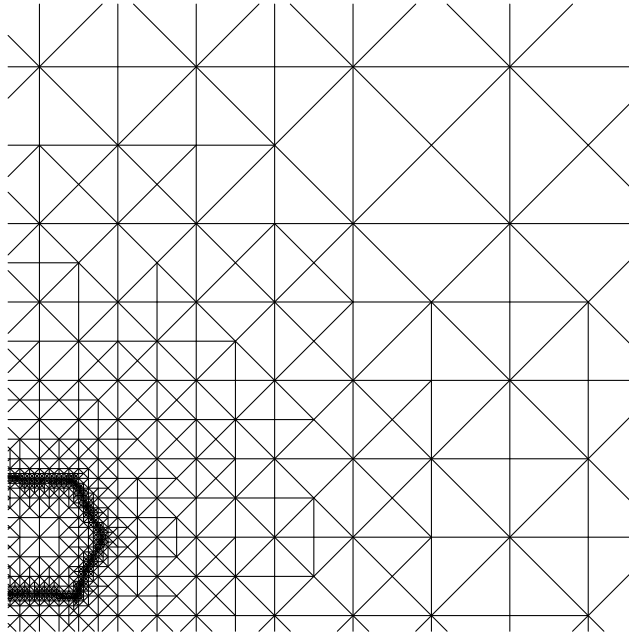
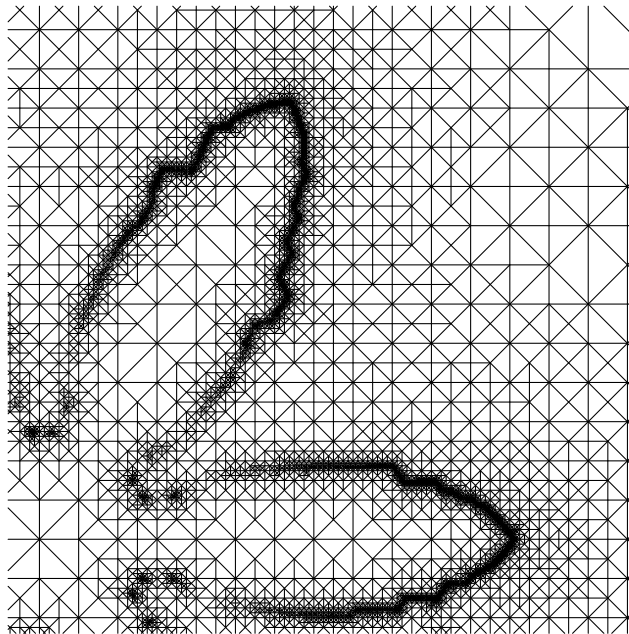**Figure 5.** Example 1 – zoom of temperature mesh at $t = 0.25$.

Figure 6. Example 1 – zoom of temperature mesh at $t = 2.0$.

The complete meshes consist of 3316 and 39942 triangles. The meshes are highly refined where the temperature gradient exhibits a large variation. This gradient varies most rapidly near fast moving parts of the interface, compare the Stefan condition (2). This results in the local refinement near the interface.

The second simulation is included to demonstrate some numerical effects, which may happen if time step size or mesh size are chosen too coarse. The simulation is done with a fixed time step size $\tau = 0.001$ and the parameter for temperature mesh adaption is $tol = 0.05$. All other parameters are the same as for the first simulation. The interface curve at time $t = 1.25$ is shown in Figure 7.
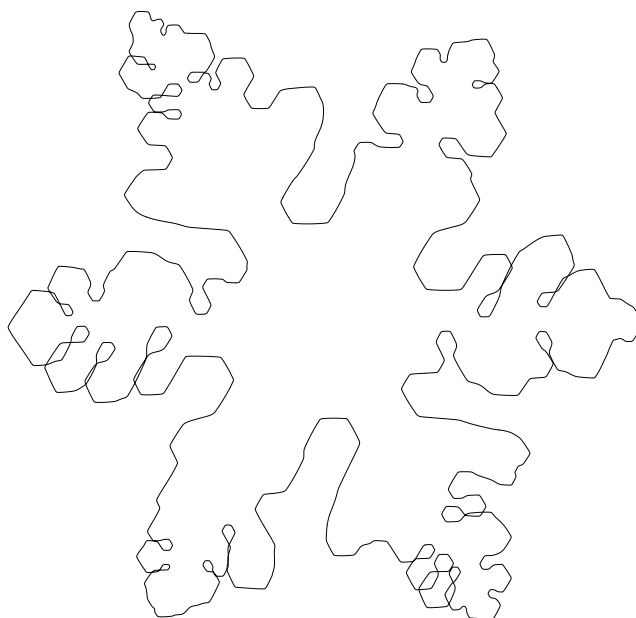

Figure 7. Example 2 – too large time steps may result in interface topology changes.

Due to the larger noise introduced by the coarser numerical approximation, side branches of the interface develop more easily. Additionally, the interface curve intersects itself, which is equivalent to a change of topology of the solid phase (the code did not check for such singularities). In our numerical experiments, such self intersections occur only when the time step size is too large; time step size reduction always eliminates such singularities.

References

1. Bänsch E., *Local mesh refinement in* 2 *and* 3 *dimensions*, IMPACT Comput. Sci. Engrg. **3** (1991), 181–191.

2. Bänsch E. and Schmidt A., *A finite element method for dendritic growth*, Computational crystal growers workshop, AMS Selected Lectures in Mathematics, (J. E. Taylor, ed.), 1992, pp. 16–20.

3. Bellettini G. and Paolini M., *Anisotropic motion by mean curvature in the context of Finsler geometry*, Hokkaido Math. J. **25** (1996), 537–566.

4. Dziuk G., *An algorithm for evolutionary surfaces*, Numer. Math. **58** (1991), 603–611.

5. _____ , *Convergence of a semi-discrete scheme for the curve shortening flow*, Math. Models Methods Appl. Sci. **4** (1994), 589–606.

6. _____ , *Discrete anisotropic curve shortening flow*, preprint, Freiburg, 1997.

7. Gage M. E., *Evolving plane curves by curvature in relative geometries*, Duke Math. J. **72** (1993), 441–466.

8. Gurtin M. E., *Toward a nonequilibrium thermodynamics of two-phase materials*, Arch. Ration. Mech. Anal. **100** (1988), 275–312.

9. Rybka P., *A crystalline motion: Uniqueness and geometric properties*, SIAM J. Appl. Math. **57** (1997), 53–72.

10. _____ , *Crystalline version of the Stefan problem with Gibbs-Thomson law and kinetic undercooling*, to appear in Advances in Diff. Equ..

11. Schmidt A., *Computation of three dimensional dendrites with finite elements*, J. Comput. Phys. **125** (1996), 293–312.

12. Taylor J. E., *Mean curvature and weighted mean curvature*, Acta metall. mater. **40** (1992), 1475–1485.

13. Taylor J. E., Cahn J. W. and Handwerker C. A., *Geometric models of crystal growth*, Acta metall. mater. **40** (1992), 1443–1474.

14. Veeser A., *Error estimates for semidiscrete dendritic growth*, in preparation.

15. Wloka J., *Partial differential equations*, Cambridge University Press.

A. Schmidt, Institut für Angewandte Mathematik, Universität Freiburg, Germany